13th World Conference on Earthquake Engineering
Vancouver, B.C., Canada
August 1-6, 2004
Paper No. 345

ON THE EFFICIENCY AND PRECISION OF ARRAY ANALYSIS OF MICROTREMORS BY THE SPAC METHOD IN PRACTICAL ENGINEERING USE

Seiji TSUNO [1] and Kazuyoshi KUDO [2]

SUMMARY

The SPatial Auto-Correlation (SPAC) method applied for array records of microtremors provides a S-wave velocity structure by surface wave inversion with sufficient accuracy. The efficiency of the SPAC method has mostly been verified for relatively deep underground structures as a tool of geophysical prospecting. However, efforts to increase its accuracy and develop the tools for measurements and analysis are still necessary for extending and applying the method in practical engineering use, especially for determining shallow velocity structures. We carried out array measurements of microtremors at 7 sites around Kanto area in Japan, where strong-motion stations have already been installed and the underground structures have been determined by other methods, such as PS logging and/or reflection survey. Through the comparison, we can conclude that the SPAC method has sufficient precision in practical engineering use.

INTRODUCTION

Conventional methods for determining a shear-wave velocity structure generally require active control sources, such as PS logging, reflection/refraction surveys, and surface wave inversion using shot-records. These methods are costly in general and sometimes meet difficulties for practical uses in urban area. On the other hand, the array observation of microtremors needs no additional sources and provides a good estimate of the S-wave velocity structure through a surface wave inversion procedure. The efficiency of the SPAC method (Aki [1]; Okada [2], [3]) applied to microtremors has mostly been verified for deep underground structures. However, the precision and guideline of the SPAC method are not sufficient to extend and apply in the field of engineering seismology and earthquake engineering, especially for shallow underground structures. The primary object for us is to understand the precision and/or limitation of the SPAC method for practical engineering use.

We carried out array observations of microtremors at 7 sites, for investigating shallow and deep S-wave velocity structures, where strong-motion stations have already been installed and the underground

[1] Graduate student, Dep. of Architecture, Graduate School of Engineering, The University of Tokyo. Email: seiji@eri.u-tokyo.ac.jp
[2] Associate professor, Earthquake Research Institute, The University of Tokyo. Email: kudo@eri.u-tokyo.ac.jp

structures have been determined by PS logging and/or reflection survey. In order to verify the efficiency of the SPAC method, we compared S-wave velocity structures estimated by this method through the inversion process with PS logging and/or reflection data directly. In the inversion procedure, we postulated that S-wave velocities increase gradually with depth, for simplicity. We also compared the site amplification factors evaluated by the estimated structural models with the spectral ratios obtained by downhole array weak-motion records, and optimized the structural models of S-wave velocity and quality factor for those spectral ratios. In addition, we tried to simulate the ground motions from downhole array records of earthquakes, based on 1-Dimensional multi-reflection theory with the estimated S-wave velocity structures by applying the SPAC method.

ARRAY OBSERVATION OF MICROTREMORS

Method

Two methods have currently been applied for obtaining a phase velocity of surface waves included in microtremors, which are the so-called, SPAC Method (Aki [1]; Okada [2], [3]) and F-K method (Capon [4]; Asten [5]; Horike [6]). If we strictly follow the theory by Aki [1], it is necessary to deploy plenty of sensors on the circumference with equi-intervals and its center in an array observation; however, Okada [7] (See Kudo [8]) proved and examined theoretically that a phase velocity of Rayleigh Waves is determined with sufficient accuracy for practical use, by arranging 4 sensors in the shape of an equilateral triangle and its center. Ling [9] suggested that a minimum wavelength of surface wave estimated by this method is 2 times of an array radius by the spatial aliasing, and Miyakoshi [10] examined by numerical analysis that an observable maximum wavelength is roughly 10 times of an array radius. Miyakoshi [10] also suggested that a minimum and a maximum wavelength estimated by the F-K method were $\sqrt{3}$ and 5 times of an array radius, respectively. On the other hand, the F-K method (Yamanaka [11]; Matsushima [12]) is superior to the SPAC method, because the F-K method allows irregularity in the array configuration. As a special case of the SPAC method, Bettig [13] has applied an extended SPAC method to the irregular array and obtained the phase velocity with reasonable accuracy. It is possible to perform the SPAC method by installing at least 3 sensors in an array observation; on the other hand, the F-K method requires at least 6-7 sensors. We used the SPAC method for obtaining a phase velocity of long wavelength by a relatively small array observation with a fewer instruments. The SPAC method has already been applied to various sites in Japan. Matsuoka [14] especially applied the SPAC method at extensive sites in the northern Kanto Plain, Japan and proposed 3-D structures. Kudo [8] also carried out array observations of microtremors quickly at the strong motion sites and damaged area in Turkey, immediately after the 1999 Kocaeli, Turkey earthquake. Detailed explanations on the SPAC methods have recently been given by Okada [3] and a short one can be found in Kudo [8].

Array Observation of Microtremors

We carried out array microtremor measurements at 7 sites around Kanto Area in Japan, for investigating the applicability of the SPAC method to shallow structures (KNS, TKD, SHS, FKSH14, SGR) and deep structures (NRT, CTS), where strong-motion stations have already been installed and the underground structures have been determined by PS logging and/or reflection survey. We deployed plural arrays by changing the radius at different observation times to obtain a phase velocity with a wide frequency range. Figure 1 shows the distribution of observation sites and Table 1 shows the summary of geotechnical data at every measurement site.

In the array observations of microtremors, we used portable instruments that consist of a tri-axial accelerometer of the highly damped moving coil type, data-logger of 24 bits resolution, time synchronization by the Global Positioning System and a signal conditioner, such as an amplifier and a filter. The sensor was developed for temporal observation of strong and weak motion of earthquakes (Kudo [15]) and its sensitivity is 1V/g and optionally 5 V/g; where, V and g denotes Volt and gravity, respectively. We usually used a single circular array consisting of four stations or a double circle array consisting of seven stations. On the other hand, we also tested the array with a scale of three times for a radius of a single array, to save measurement time and to use roads having rectangular corners for practical convenience in populated area. The array configuration is shown in Figure 2-a. Figure 2-b shows a range of wavelength (WL) possible to estimate phase velocities by the proposed array configuration (e.g. radius (R) =100, 300 and 900m), according to 2R<WL<10R (Ling [9]; Miyakoshi [10]).

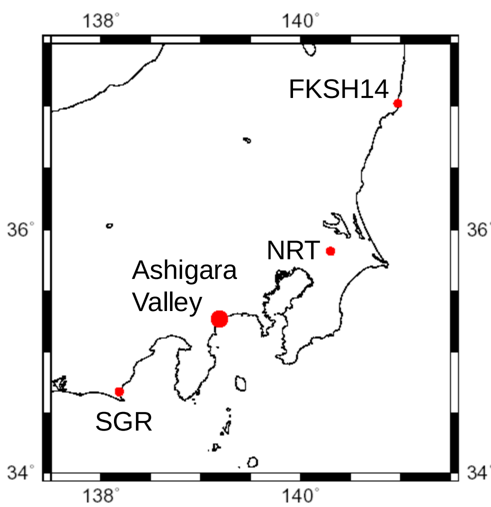

Figure 1 Location map showing array observation sites of microtremors. Large red circle represents the four sites such as KNS, TKD, SHS and CTS in Ashigara Valley, Kanagawa Prefecture.

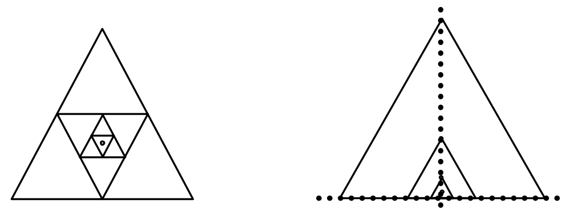

(a) Two different array configurations
The orthodox type (Okada; left) and the proposed conventional type (right) are shown.

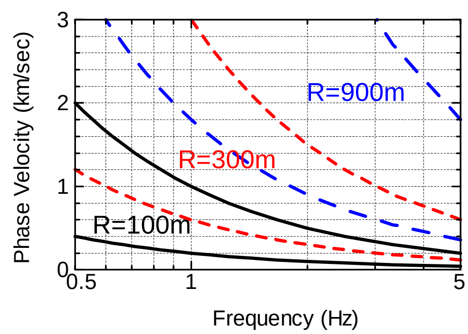

(b) A range of wavelength (WL) possible to estimate phase velocities by the proposed array configuration (R=100, 300 and 900m) according to 2R<WL<10R.

Figure 2 Proposed array configuration and its ability.

Table1 Summary of geotechnical data at observation sites.

A reflection survey was carried out in the vicinity NRT by NIED, and no geological/geotechnical investigation was performed at SGR. National Research Institute for Earth Science and Disaster Prevention (NIED) maintains FKSH14 and NRT stations, and Earthquake Research Institute (ERI) maintains the other stations.

Station	Latitude(N)	Longitude(E)	Logging	P-Reflection	Depth of Sensors installed
KNS (Kuno)	35.2666	139.1516	PS (101m)	—	GL - 0, 30, 100m
TKD (Takada)	35.2847	139.1947	PS (40m)	—	GL - 0, 40m
SHS (Seisyo)	35.2715	139.1891	PS (70m)	—	—
FKSH14 (Taira)	37.0233	140.9736	PS (150m)	—	GL - 0, 150m
SGR (Sagara)	34.675	138.1833	—	—	GL - 0, 250m
CTS (Kamonomiya)	35.2746	139.1915	PS (498m)	—	GL - 0, 10, 30, 100, 467m
NRT (Narita)	35.8275	140.3013	Sonic (1336m)	4000m	GL - 0, 1295m

Analysis

We used records of array microtremors that have relatively high power and good coherence, by excluding traffic and impulsive noises near sensors. We also determined time-blocks of array records in data processing, according to the array sizes and the frequency range to analyze. Figure 3, for instance, shows integrated velocity waveforms of microtremors and the obtained phase velocities by applying the SPAC method at NRT. The phase velocities are determined using different sizes of arrays so as to overlap successively versus frequency. We regarded the circles shown in Figure 3-b as the target phase velocity in inversion process, which corresponds to $C_o(T_i)$ in equation (1). We obtained the phase velocity by fitting the SPAC coefficients to Bessel function versus distance, which is called the E-SPAC method (Ling [16]). Figure 4 shows examples by the E-SPAC method at NRT for some representative frequencies.

We used the genetic algorithm (GA; Yamanaka [18]) for surface wave inversion, postulating that S-wave velocities increase gradually with depth, for simplicity. We also inverted the structural model including a thin high velocity at TKD, for understanding the influence of the assumption to the estimated S-wave velocity structure. We performed GA several times by giving different parameters (search area) and/or different number of layers. We also repeated the process with same search area by generating five different random numbers. We selected the best result such that the error defined in equation (1) becomes minimum, as S-wave velocity structure at an array observation site.

$$Error = \frac{1}{L}\sum_{i=1}^{L}\left[C_o(T_i) - C_t(T_i)\right]^2 \qquad (1)$$

$C_o(T_i)$: *Observed phase velocity*

$C_t(T_i)$: *Theoretical phase velocity*

Where, T_i, L denote period and its number in inversion process, respectively.

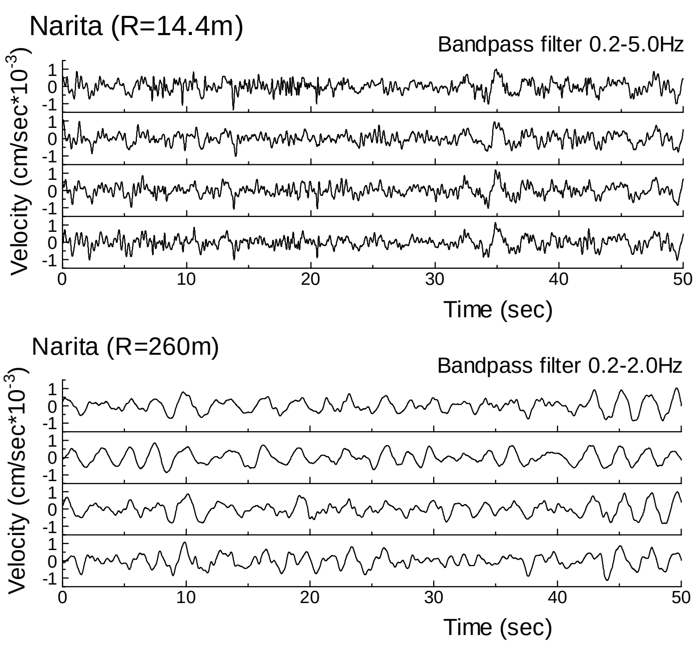

(a) Velocity waveforms in array radii of 14.4m (upper) and 260m (lower) at NRT site, which are processed by bandpass filter of Butterworth type, are shown.

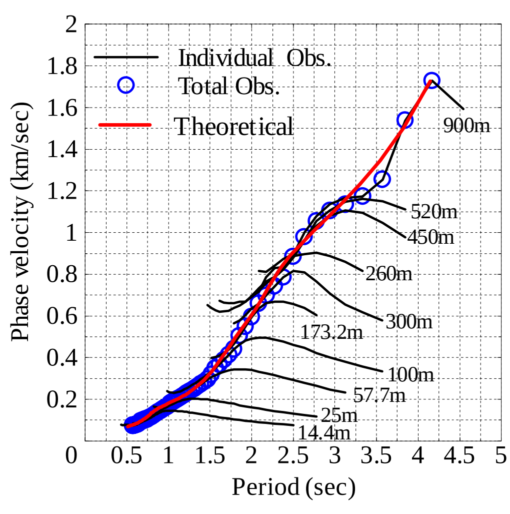

(b) The phase velocities determined by ten different array distances are shown in fine solid lines. The target phase velocity obtained by the E-SPAC method and the theoretical one calculated by Haskell [17] are also shown by circle and thick line, respectively.

Figure 3 Records of array microtremors and the obtained phase velocities at NRT.

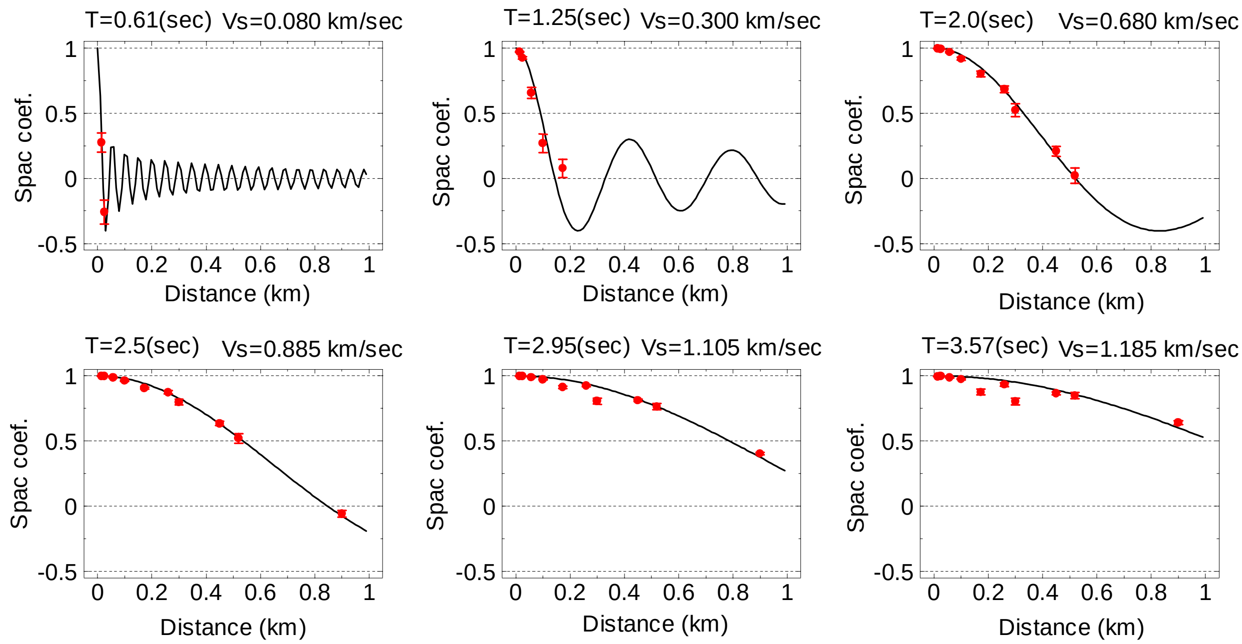

Figure 4 Examples of the SPAC coefficients fitted to the Bessel function at NRT for some representative frequencies. The error bars indicate the means of SPAC coefficients and their standard deviations determined using from 15 to 30 time-blocks, respectively.

RESULTS AND VERIFICATION BY LOGGING DATA

Shallow and deep S-wave velocity structures estimated by the SPAC method are shown in Figure 5 and 6, respectively. The estimated velocity structures for the shallow sites (<100m) at KNS, TKD, SHS and FKSH14 are compared with the geotechnical profiles by logging data. The deep ones at NRT and CTS are also compared with logging data and/or result of reflection survey. The location of array microtremors measurement at NRT is about 2km distant from the borehole (Suzuki [19]). On the other hand, the line of reflection survey (Kasahara [20]) crosses the array area of microtremors measurement and a part of it was close to the borehole site. A small difference of basement depth is found between array observation area and logging point as revealed in the reflection survey result, as shown in Figure 6-e. In order to determine S-wave velocity structure at logging point, we also estimated the structural model included a high velocity layer (Vp 5.0km/sec) overlying on basement. So far, SGR site have no geotechnical data.

The geological interfaces for shallow underground structures estimated by the SPAC method are slightly different from those determined by PS loggings. The differences appear at depths of a thin high and/or low velocity in the middle of layers. However, we confirmed modest agreements between the estimated structural models and the results of PS logging as shown in Figure 5. The postulation that S-wave velocities increase gradually with depth gives only an equivalent S-wave velocity structure; however, the observed phase velocity dispersion of Rayleigh Waves agrees fairly, as shown in Figure 7. We also confirmed that the estimated deep structures match quite well with the other results, such as PS-logging and reflection survey even for depths of geological interface. We obtained the phase velocity for long period with sufficient accuracy, so that the estimated depth of basement at NRT agreed quite well with the result of reflection survey as shown in Figure 6-e. However, in case that the phase velocity is not available for long period range by array observations of microtremors, we are obliged to assume a depth and/or a velocity of basement on the basis of geological or gravitational information.

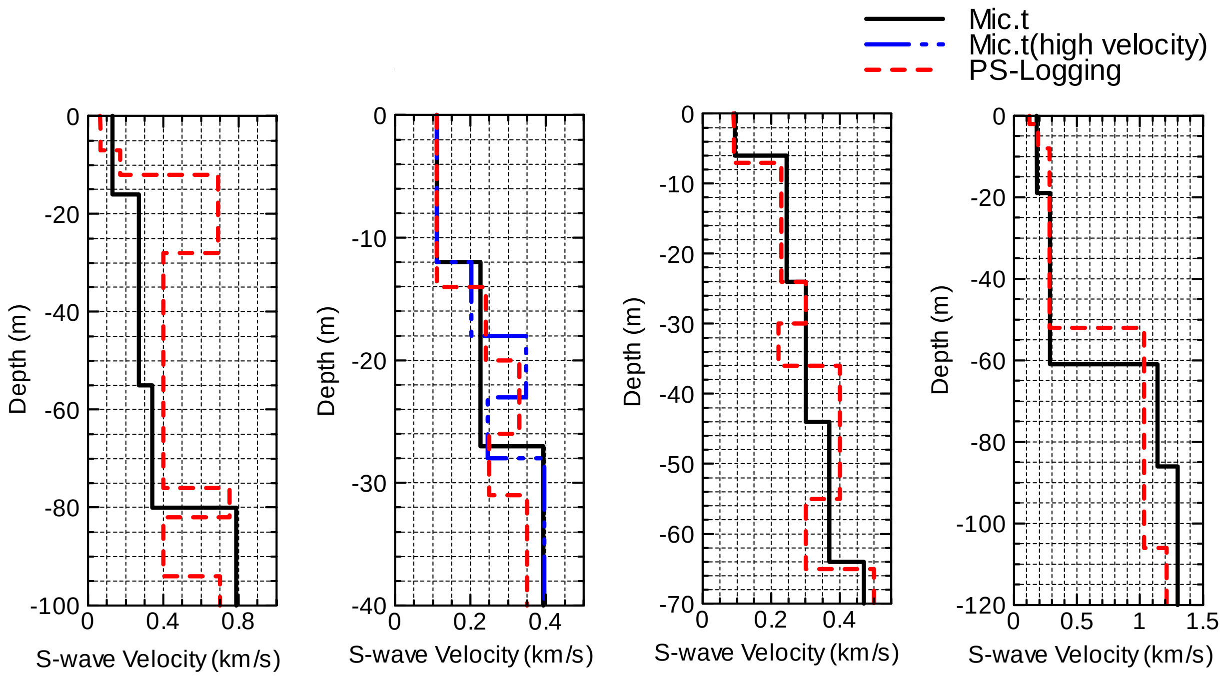

(a) KNS (b) TKD (c) SHS (d) FKSH14

Figure 5 Comparison of S-wave velocity structures estimated by array microtremors with the logging data, for the site of shallow underground structures. The structural model at TKD included a thin high velocity was estimated by all owing velocity conversion in the layers.

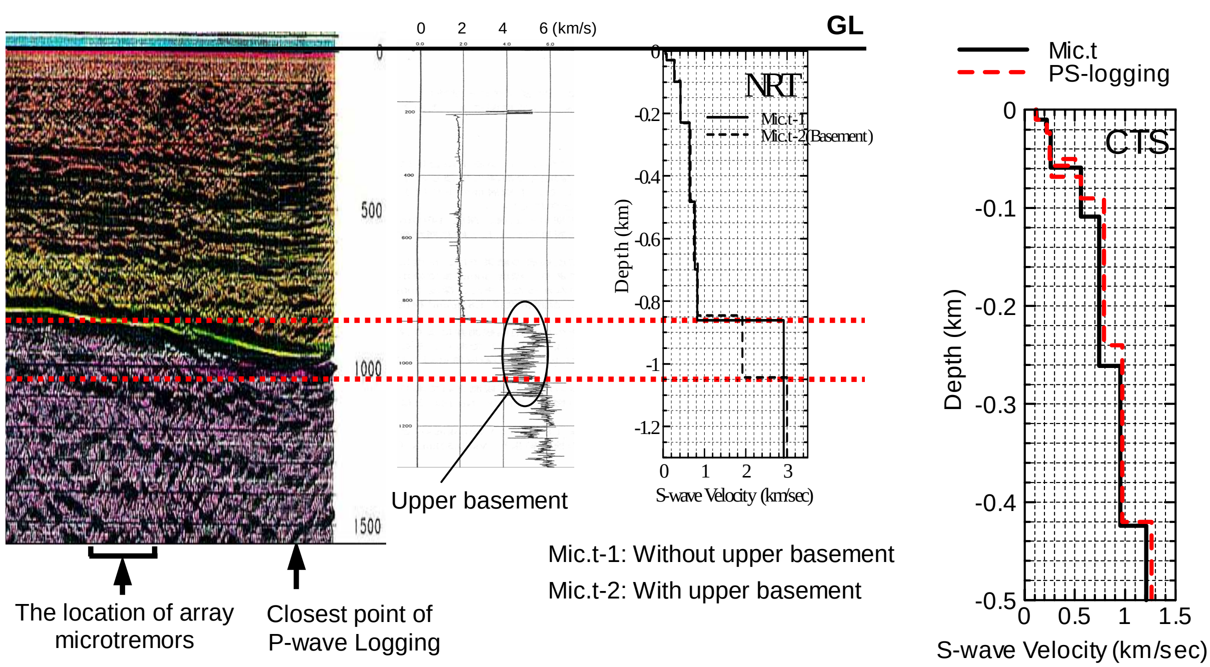

(e) Comparison of S-wave velocity structure determined by the SPAC method (right) with Sonic-logging data (Suzuki [19]; middle) and reflection survey result (Kasahara [20]; left) in NRT.

(f) CTS

Figure 6 Comparison of S-wave velocity structures for deep underground structure (NRT and CTS) estimated by array microtremors with logging data and/or result of reflection.

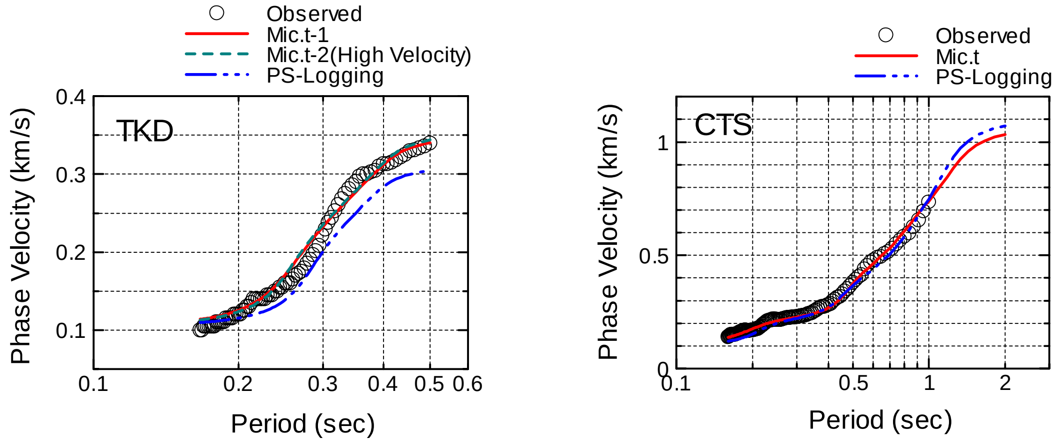

(a) TKD (b) CTS

Figure 7 Comparison of the phase velocities calculated by the estimated S-wave velocity structures and the logging data with observed one at TKD and CTS.

VERIFICATION OF THE SITE AMPLIFICATION FACTOR USING EARTHQUAKE GROUND MOTION

The site amplification factor evaluated by the geotechnical data does not necessarily agree with that estimated by earthquake motion, due to inhomogeneous or inclined layers, anisotropy and so on. The primary purpose in the field of earthquake engineering is to evaluate the site characteristics of amplification and attenuation effects. We verified the site characteristics evaluated by the estimated S-wave velocity structures using weak-motion records of earthquakes to understand the precision and/or limitation of the SPAC method for practical use.

Empirical site amplification factor

In this study, the array observations of microtremors were carried out in and around strong-motion stations with a borehole array, except SHS site. We evaluated the empirical site characteristics by the surface/downhole horizontal spectral ratios using the early arrivals of S-waves in the earthquake records. We generally selected the records of intermediate to deep earthquakes, deeper than 30km, in order to eliminate the variations of incident angle of input motions. We used a time window of about 3-5 sec for the early part of S-wave to obtain spectral ratios for shallow profiles. On the other hand, we used the ground motion records of earthquakes larger than magnitude (Mj) 5 with a time window of 5-10 sec for deep ones, aiming to discuss the site characteristics in a wide period range. Table 2 shows the earthquake data used to obtain the spectral ratios. We used the transverse component to calculate the spectral ratio at SGR, where short distance records were mostly retrieved. We computed separately the spectral ratios for both NS and EW components at KNS, due to remarkable differences of those spectral ratios in the two components. Kudo [21] reported that those differences are caused by an effect of an anisotropy in the middle layer of 30-80m depths, although 2-D/3D effects were also indicated (Satoh [22]; Sato [23]). We corrected the polarity of records by maximizing the correlation coefficient between surface and downhole motions (Kato [24]), in case the polarity of sensors in a borehole is not clearly identified.

Verification of the site amplification factors evaluated by the estimated models

We compared the site amplification factors calculated by the estimated S-wave velocity structures with the observed spectral ratios, which are based on 1-Dimensional multi-reflection theory assuming vertical incident of SH-wave. Figure 8 and 9 shows the comparisons of the spectral ratios that are computed using two structure models by microtremors and PS-logging with those of the observations. In this analysis, we controlled the quality factors of frequency dependence by forward modeling applied to the observed spectral ratios.

The site amplification factors by the estimated shallow S-wave velocity structures agree well for first and second peak frequencies and its amplitudes with the empirical ones. On the other hand, the site amplification factors by logging data show better agreements with the empirical ones even for the higher frequency than 5Hz. It is difficult to discriminate whether that difference is caused by the approximation that S-wave velocities increase with depth or by insufficiency of resolution for shallow structure. Topographic effects and lateral heterogeneity of surface layers may also cause the discrepancies. However, site amplification factors higher than 5Hz have less importance for assessing earthquake-resistant reliability of ordinary buildings in Japan. Therefore, we presume that the SPAC method with simple inversion procedures has adequate accuracy for characterizing the site effects for engineering purpose. We also confirmed that dominant frequencies and shapes of site amplification factors by the estimated deep structures agree well for periods longer than 1sec with observed ones. The SPAC method has enough efficiency for investigating deep underground structures, which are important for assessing large-scale man-made structures against earthquakes.

Optimization of the estimated models

We applied optimization technique to determine the S-wave velocity, depth and quality factor using the observed spectral ratios. In the optimization, we minimized the residuals between observed spectral ratios $A_o(f_i)$ and the theoretical ones $A_t(f_i)$ by a quasi-Newton method (Satoh [24]), giving weight to long period contents, as shown in the equation (2). We optimized S-wave velocity and depth at first, considering the spectral ratios in and around dominant frequencies. Next, we also repeated this process for optimizing the quality factor (Q_0) of frequency dependence in the form of $Q=Q_0 f^a$. However, we fixed a = 0.7 for Vs<700m/sec and a = 0.5 for Vs>700m/sec, respectively.

$$J(r) = \sum_{i=1}^{n} \frac{\{\log A_o(f_i) - \log A_t(f_i : r)\}^2}{1/(\log f_i - \log f_{i-1})} \qquad (2)$$

Where, f_i, n denote frequency and its number, respectively.

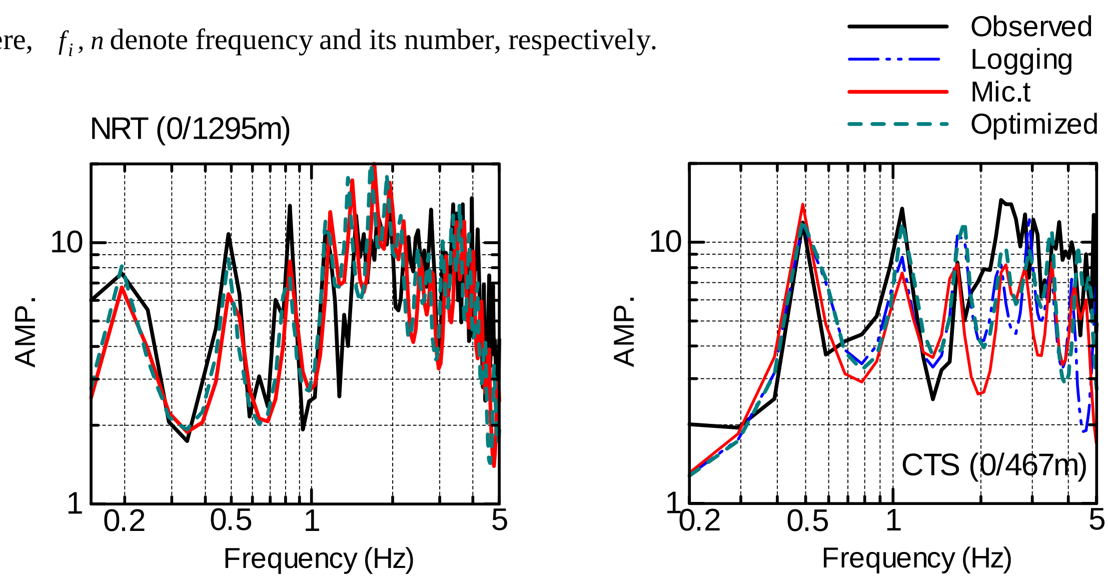

(a) NRT (GL/1295m)　　(b) CTS (GL/467m)

Figure 8 Comparison of the site amplification factors by array microtremors and logging data with the empirical ones using earthquake motions, for the site of deep underground structures (NRT and CTS). The site amplification factors by the optimized structural models are shown, simultaneously.

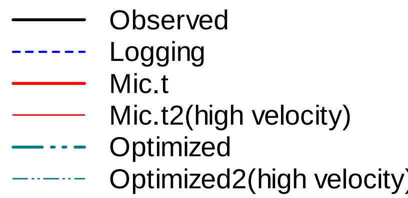

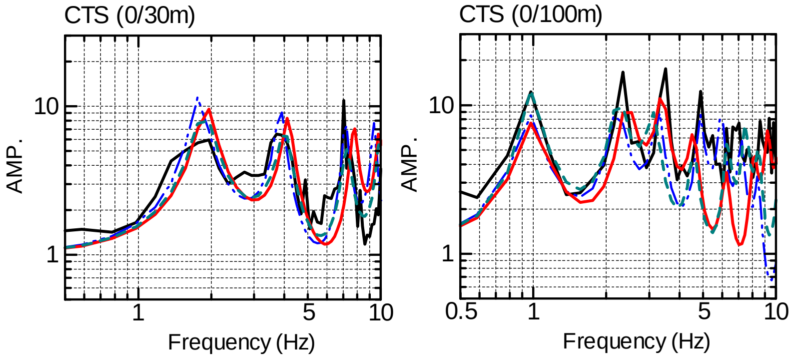

(c) CTS (The sensors are installed at 5 different depths in this station. The site amplification factor by spectral ratio of GL/467m depth is also shown in Figure 8-b.)

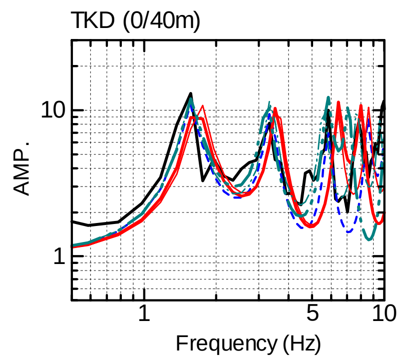

(d) TKD (The site amplification factors by the estimated velocity structural models included a thin high velocity are shown.)

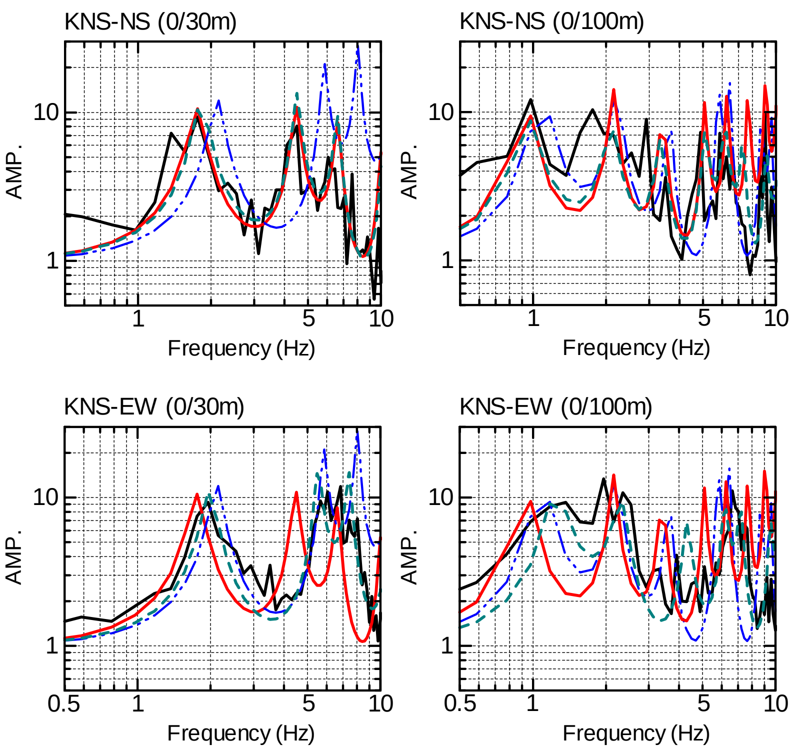

(f) KNS (The site amplification factors for NS and EW components are shown on upper and lower figures, respectively. An anisotropic medium in the middle layer is pointed out in this site. We confirmed that the observed spectral ratios for NS and EW components have a remarkable difference with each other. We also confirmed that the site characteristics by array microtremors and logging data correspond to the observed ones for NS and EW component, respectively.)

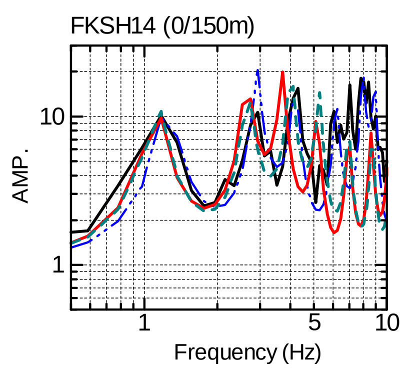

(e) FKSH14

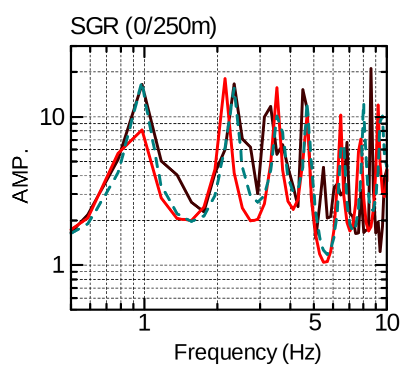

(g) SGR (No geotechnical survey has been carried out.)

Figure 9 Comparison of the site amplification factors by array microtremors and logging data with the empirical ones using earthquake motions, for shallow underground structures (CTS, TKD, FKSH04, KNS and SGR). The site amplification factors by the optimized structural models are shown, simultaneously.

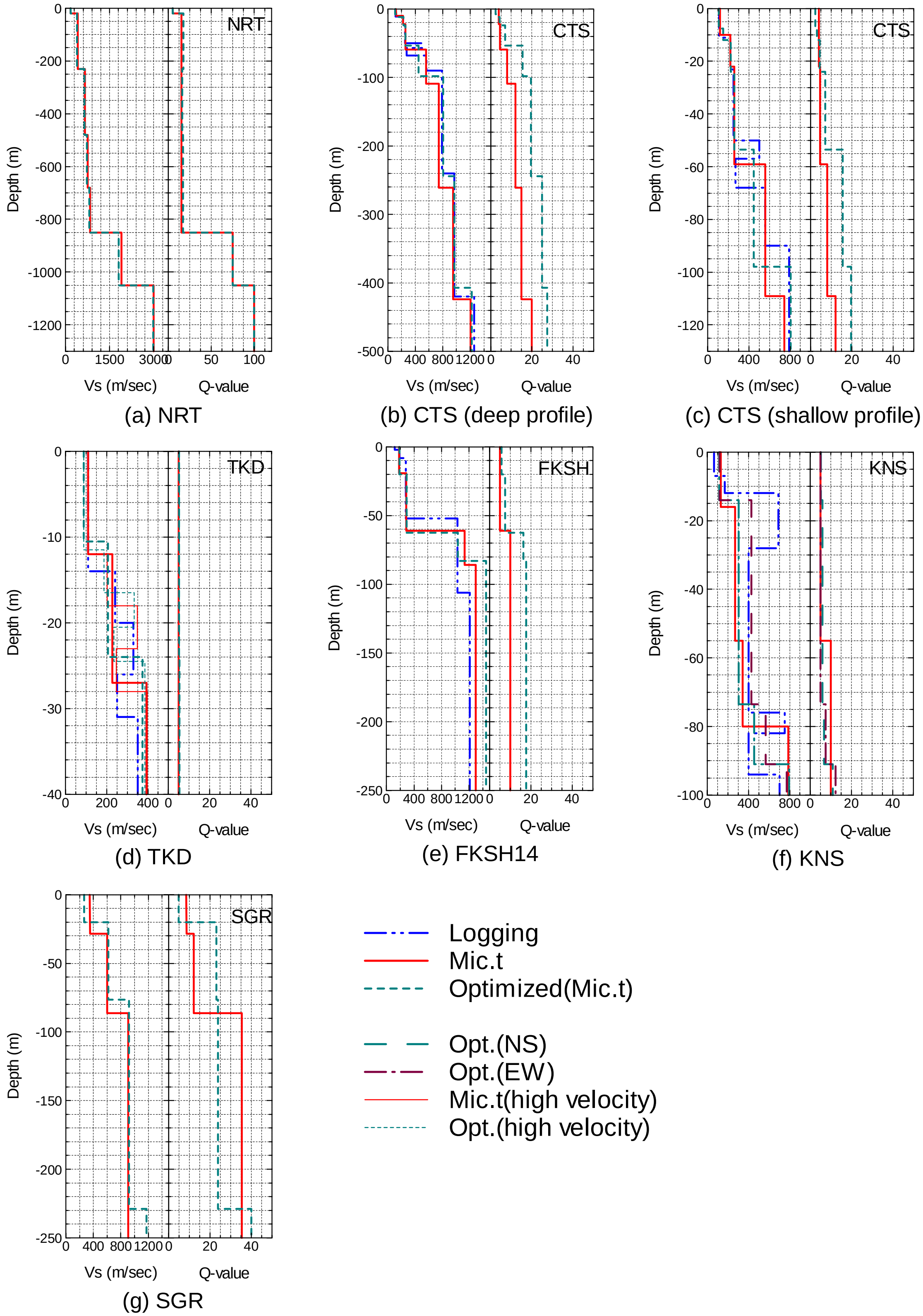

Figure 10 S-wave velocity and Quality factor structures at array observation sites are shown. At KNS, the structural models for NS and EW component are shown. The structural model including a thin high velocity is estimated at TKD. We compared the estimated structures with optimized ones for both deep (b) and shallow (c) structures at CTS.

Table 2 The earthquakes used to obtain the surface/downhole spectral ratios at each station. The hypocenter locations are provided by Feesia system in National Research Institute for Earth Science and Disaster Prevention.

KNS (Kuno)

Earthquake location	Origin time	Latitude (N)	Longitude (E)	Depth (km)	Mj
North-West Chiba	1999/9/13/07:57	35.6	140.2	80	5.1
East Yamanashi	2000/2/11/20:57	35.5	139	20	4.4
West Kanagawa	2000/5/2/23:33	35.3	139.1	10	3.7
North-East Chiba	2000/6/3/17:55	35.7	140.8	50	5.8
Off Ibaragi	2000/7/21/03:40	36.6	141	50	6.1
East Kanagawa	2000/9/29/08:56	35.5	139.7	90	4.6
West Kanagawa	2001/2/2/8:10	35.5	139.1	10	4.4
Middle Shizuoka	2001/4/3/23:57	35	138.1	30	5.3
South Chiba	2001/4/10/10:04	35.3	140.4	100	4.7
South Ibaragi	2001/7/20/06:03	36.2	139.8	60	5.1
West Kanagawa	2001/12/8/04:07	35.5	139.1	30	4.6

TKD (Takada)

Earthquake location	Origin time	Latitude (N)	Longitude (E)	Depth (km)	Mj
North-West Chiba	1999/9/13/07:57	35.6	140.2	80	5.1
North-East Chiba	2000/6/3/17:55	35.7	140.8	50	5.8
Off Ibaragi	2000/7/21/03:40	36.6	141	50	6.1
East Kanagawa	2000/9/29/08:56	35.5	139.7	90	4.6
Middle Shizuoka	2001/4/3/23:57	35	138.1	30	5.3

FKSH14 (Taira)

Earthquake location	Origin time	Latitude (N)	Longitude (E)	Depth (km)	Mj
Off Ibaragi	2000/7/21/03:39	36.6	141	50	6.1
Torishima waters	2000/8/6/16:28	28.9	140.1	430	7.3
Off Fukushima	2000/11/16/18:31	37.5	141.6	60	5.3
Off Ibaragi	2001/9/4/23:54	36.8	141.5	40	5.4
Off Fukushima	2001/10/2/17:20	37.7	141.9	40	5.6
South Iwate	2001/12/2/22:02	39.4	141.3	130	6.3

SGR (Sagara)

Earthquake location	Origin time	Latitude (N)	Longitude (E)	Depth (km)	Mj
West Shizuoka	2001/2/23/7:23	34.8	137.5	50	5.3
Middle Shizuoka	2001/4/3/23:57	35	138.1	30	5.3
Middle Shizuoka	2001/6/1/00:41	35	138.1	40	4.8
Middle Shizuoka	2001/6/3/11:33	35	138.1	40	4.3

CTS (Kamonomiya)

Earthquake location	Origin time	Latitude (N)	Longitude (E)	Depth (km)	Mj
North-East Chiba	2000/6/3/17:55	35.7	140.8	50	5.8
Off Ibaragi	2000/7/21/03:40	36.6	141	50	6.1
Torishima waters	2000/8/6/16:29	28.9	140.1	430	7.3
West Kanagawa	2001/2/2/8:10	35.5	139.1	10	4.4
South Iwate	2001/12/2/22:02	39.4	141.3	130	6.3
West Kanagawa	2001/12/8/04:07	35.5	139.1	30	4.6

NRT (Narita)

Earthquake location	Origin time	Latitude (N)	Longitude (E)	Depth (km)	Mj
Off Fukushima	1998/4/9/17:45	36.9	141	93	5.4
Off Ibaragi	2000/7/21/03:40	36.6	141	50	6.1
Torishima waters	2000/8/6/16:28	28.9	140.1	430	7.3
Off Ibaragi	2000/12/5/1:47	35.8	141.2	37	5.3

Figure 8 and 9 shows the comparisons of site amplification factors by the initial and the optimized structural models with those of the observations at 6 sites, focusing on deep velocity structures (NRT and CTS) and shallow ones (CTS, TKD, FKSH04, KNS and SGR), respectively. The optimized models are shown in Figure 10, with the initial models. The differences in velocity and in thickness of layers between initial and optimized models were mostly less than 15% against the optimized one. It is especially small, within 5%, at NRT. We also compared the simulated surface motion computed from downhole earthquake records based on 1-Dimensional multi-reflection theory in time domain, using the estimated S-wave velocity structures. The observed surface ground motions of earthquakes and the simulations agree well at least for the early part of the S-wave, as shown in Figure 11. We can conclude that the phase characteristics are also well predicted using the structural models estimated by the SPAC method.

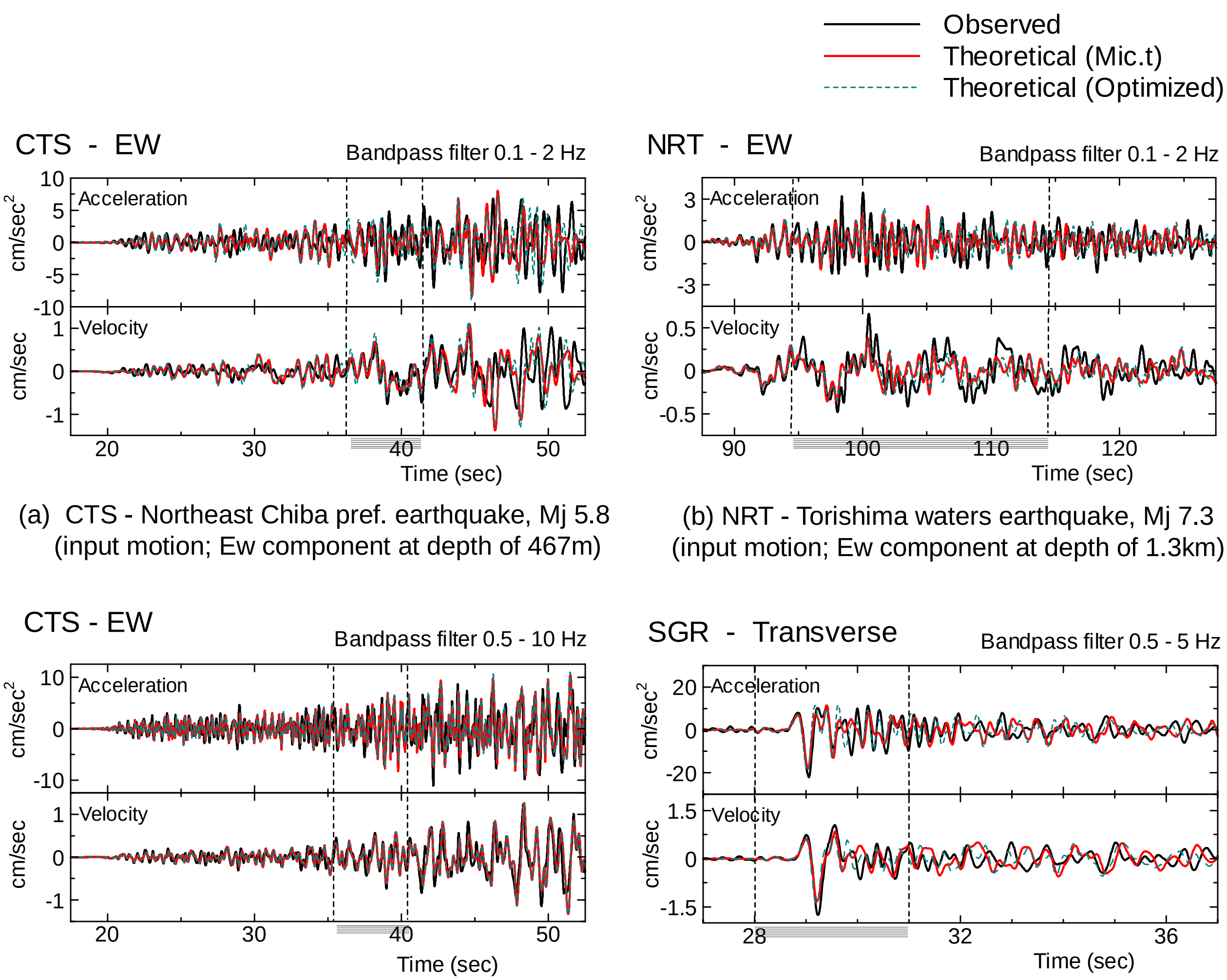

(a) CTS - Northeast Chiba pref. earthquake, Mj 5.8 (input motion; Ew component at depth of 467m)

(b) NRT - Torishima waters earthquake, Mj 7.3 (input motion; Ew component at depth of 1.3km)

(c) CTS - Northeast Chiba pref. earthquake, Mj 5.8 (input motion; Ew component at depth of 30m)

(d) SGR - Western Sizuoka pref. earthquake, Mj 4.9 (input motion; Trans. component at depth of 250m)

Figure 11 Simulated ground motions (acceleration and velocity waveforms) using downhole records are shown, with the observations. Input motions were given at depth of 30m (a) and 467m (c) for CTS, at 250m for SGR and at 1295m for NRT, respectively. The shade parts in these figures show a time window of an early arrival of S-wave used in the calculation for obtaining a surface/downhole horizontal spectral ratio.

DISCUSSION

We compared the site amplification factors by the estimated structural models, PS-logging and the optimized models with the empirical spectral ratios. Figure 12 and 13 shows the comparisons of dominant (first and second peak) periods and its amplitudes with three sets of data pairs, respectively. The matching among all combinations is satisfactory. In more detail, the agreement of both peak periods and its amplification factors between logging data and optimized models is best among others. The reason for the small inferiority of the models by the SPAC method will be that the estimated S-wave velocity structure is an average for the array spaces and is an approximation neglecting thin high or low velocity layers. However, differences among 3 types of structural models are very small as it is difficult to distinguish which simulation based on the optimized or the initial model (result by the SPAC method) fits the observation better, as shown in Figure 11. We estimated two different S-wave velocity structures at TKD, an approximate model by assuming a S-wave velocity increasing gradually with depth (solid line in Figure 5-b) and another model including thin high and/or low velocity layers (a dotted line in Figure 5-b). The site amplification factors by the approximate model agree well for a frequency range lower than 5 Hz with another model, as shown in Figure 9-d. We infer that both peak periods and its amplification factors are well predicted by the SPAC method, introducing simplicity in inversion procedures, for practical use.

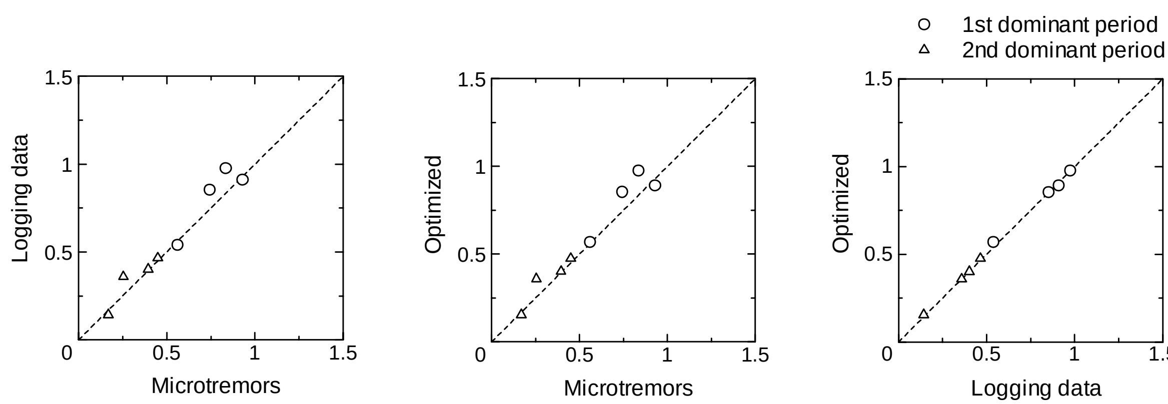

(a) Microtremors VS PS-logging (b) Microtremors VS Optimized (c) PS-logging VS Optimized

Figure 12 Comparison of the peak periods of 1D response among the estimated structural models by the SPAC method, PS-logging data and the optimized models. 1D response is estimated by vertically propagating incident SH-wave.

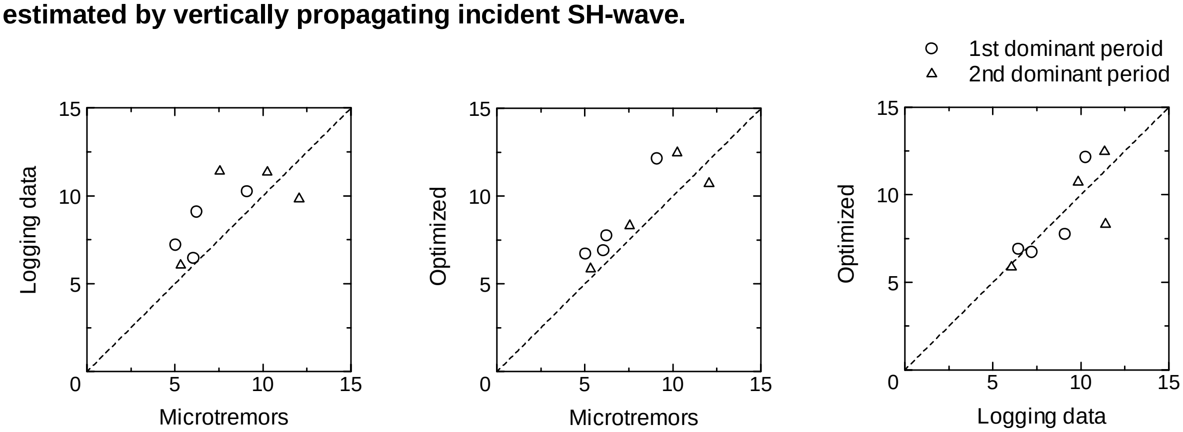

(a) Microtremors VS PS-logging (b) Microtremors VS Optimized (c) PS-logging VS Optimized

Figure 13 Comparison of the amplification factors of 1D response among the estimated structural models by the SPAC method, PS-logging data and the optimized models.

CONCLUSION

In order to verify the precision and limitation of the SPAC method, we carried out array observations of microtremors at strong-motion stations, where a borehole accelerograph array has been installed and/or the underground structures are determined by the other methods, such as PS logging and reflection survey. The approximation, that S-wave velocities increase gradually with depth in an inversion procedure, is certainly inaccurate since it is difficult to estimate details of the interface of a layer, especially in cases where a thin high and/or low velocity layer is included. However, the site amplification factors by the estimated shallow S-wave velocity structures agree well with peak frequencies and amplitudes in frequencies lower than 5Hz. The reason for the validity of approximation is that the surface wave inversion gives an equivalent S-wave velocity structure even for vertical traveling waves. In addition, interposed thin high and/or low velocity layers may not have significant effects on frequencies lower than 5 Hz. On the other hand, the estimated deep structures were in good agreement even for the geological interfaces with PS logging and with the result of reflection survey. The differences in velocity and in thickness of layers between the estimated structural models and the optimized models determined by spectral ratios were mostly less than 15%. We also simulated well the surface ground motions using downhole array records of earthquakes, based on 1-D multi-reflection theory applying the estimated structures. We conclude that S-wave velocity structures estimated by the SPAC method with simple inversion procedures have sufficient precision for practical engineering use in predicting both peak frequency and amplitude.

ACKNOWLEDGMENT

We used the earthquake records of Kik-net, NRT and the other data provided by National Research Institute for Earth Science and Disaster Prevention. The other sites have been maintained by Earthquake Research Institute (ERI), the University of Tokyo. Surface logging data by Nuclear Power Engineering Corporation and ERI are used. We are also grateful for all the people who were helpful for acquiring data, especially Prof. Sigeo Kinoshita. We also thank Dr. Tatsuo Kanno, Mr. Sos S. Margaryan and other people who helped us for conducting array observations of microtremors.

REFERENCES

1. Aki K. “Space and time spectra of stationary stochastic waves, with special reference to microtremors” Bull. Earthq. Res. Inst. 35, 1957: 415-456.
2. Okada H. “Microtremors as exploration method, Geo-exploration handbook” Soc. Exploration Geophysicists of Japan 2, 1998: 203-211 (in Japanese).
3. Okada H. “The microtremor survey method (Geophysical monograph series, No. 12)”, Society of Exploration, 2003.
4. Capon J. “High-resolution frequency-wavenumber spectrum analysis” Proc. IEEE 57, 1969: 1408-1418.
5. Asten M, Henstridge J D. “Array estimators and the use of microseisms for reconnaissance of sedimentary basin” Geophysics 49, 1984: 1828-1837.
6. Horike M. “Inversion of phase velocity of long-period microtremors to S-wave-velocity structure down to the basement in urbanized area” J. Phys. Earth 33, 1985: 59-96.
7. Okada H. “Remarks on the efficient number of observation points for the spatial auto-correlation method applied to array observations of microtremors” Proc. of the 104th SEGJ Conf., Society of Exploration Geophysicists, Japan, 2001: 26-30 (in Japanese).
8. Kudo K, Kanno T, Okada H, Ozel O, Erdik M, Sasatani T, Higashi S, Takahashi M, Yoshida K. “Site-specific issues for strong ground motions during the Kocaeli, Turkey, Earthquake of 17

August 1999, as inferred from Array Observations of Microtremors and Aftershocks" Bull. Seism. Soc. Am. 92, 2002: 448-465.
9. Ling S, Matsushima T, Okada H. "An exploration method using microtremors (6) Determination of the effective frequency range in the Spatial Autocorrelation Method" Proc. of the 85th SEGJ Conf., Society of Exploration Geophysicists, Japan, 1991: 261-263 (in Japanese).
10. Miyakoshi K. "A range of wavelengths possible to estimate phase velocities of surface waves in microtremors" Proc. of the 94th SEGJ Conf., Society of Exploration Geophysicists, Japan, 1996: 178-182 (in Japanese).
11. Yamanaka H, Takemura M, Ishida H, Ikeura T, Nozawa T, Sasaki T, Niwa M. "Array measurement of long-period microtremors and estimation of S-wave velocity structure in the western part of Tokyo metropolitan area" Journal of the Seismological Society of Japan 47, 1994: 163-172 (in Japanese).
12. Matsushima T, Okada H. "Determination of deep geological structures under urban areas" BUTSURI-TANSA 43, 1990: 21-33 (in Japanese).
13. Bettig B, Bard P Y, Scherbaum F, Riepl J, Cotton F, Cornou C, Hatzfeld D. "Analysis of dense array noise measurements using the modified spatial auto-correlation method (SPAC): application to the Grenoble area" Boll. Geof. Teor. Appl. 42, 2001: 281-304.
14. Matsuoka T, Shiraishi H. "Application of an exploration method using microtremor array observations for high resolution surveys of deep geological structures in Kanto plains –Estimation of 3-D S-wave velocity structure in the southern part of Saitama prefecture-" BUTSURI-TANSA 55, 2002: 127-143 (in Japanese).
15. Kudo K, Takahashi M, Sakaue M, Kanno T, Kakuma H, Tsuboi D. "A highly over-damped moving coil type accelerometer for mobile strong motion observation and its performance tests", Report of Grant-in-Aid for Scientific Research-07558056, 1998 (in Japanese with English abstract).
16. Ling S, Okada H. "An extended use of the spatial autocorrelation method for the estimation of geological structure using microtremors" Proc. of the 89th SEGJ Conf., Society of Exploration Geophysicists, Japan, 1993: 44-48 (in Japanese).
17. Haskell N A. "The dispersion of surface wave on multilayered media" Bull. Seism. Soc. Am. 43, 1953: 17-34.
18. Yamanaka H, Ishida H. "Application of genetic algorithms to an inversion of surface-wave dispersion data" Bull. Seism. Soc. Am. 86, 1996: 436-444.
19. Suzuki H, Omura K. "Geological and logging data of the deep observation wells in the Kanto region, Japan" Technical Note of the National Research Institute for Earth Science and Disaster Prevention 191, 1999 (in Japanese).
20. Kasahara K, Kawasaki S, Ikawa T, Kawanaka T. "Deep seismic reflection survey using Vibroseis in the northern part of Narita City, Kanto basin, Japan" Abstracts 2001 Japan Earth and Planetary Science Joint Meeting, 2001: Sz-P001 (in Japanese).
21. Kudo K, Sawada Y. "A brief review on Ashigara valley blind prediction test and some follow-up studies" The Effects of Surface Geology on Seismic Motion, Volume 1:A.A.Balkema, 1998: 305-312.
22. Satoh T, Sato T, Kawase H. "Nonlinear behavior of soil sediments identified by using borehole records observed at the ashigara valley, Japan" Bull. Seism. Soc. Am. 85, 1995: 1821-1834.
23. Sato K, Higashi S, Yajima H, Sasaki S. "Ashigara valley test site, 1D or 2D/3D?" The Effects of Surface Geology on Seismic Motion, Volume 1: A.A.Balkema, 1998: 319-340.
24. Kato K, Yamazoe M, Takemura M. "Azimuth estimation of Kik-net borehole seismometers distributed in Cyugoku and Shikoku regions, Japan -On the basis of strong motion records from the Tottoriken-seibu and the Geiyo earthquakes-" Journal of the Seismological Society of Japan 54, 2001: 421-429 (in Japanese).